Precise Optical Measurement of Lamb Shifts in Atomic Hydrogen

D. J. Berkeland, E. A. Hinds, and M. G. Boshier
Physics Department, Yale University, P.O. Box 208120, New Haven, Connecticut 06520-8120
(Received 27 April 1995)

We have measured the combination of hydrogen Lamb shifts $\mathcal{L}_{1S} - 5\mathcal{L}_{2S} + 4\mathcal{L}_{4P}$ by comparing the frequencies of the $1S$-$2S$ and $2S$-$4P$ transitions. The measurement determines the $1S$ Lamb shift to be 8 172 827(51) kHz, the most precise value for any Lamb shift. The theoretical predictions for $\mathcal{L}_{1S}$ are 8 172 802(30) and 8 172 654(40) kHz, corresponding to proton charge radius values of 0.862(12) and 0.805(11) fm, respectively.

PACS numbers: 32.30.Jc, 06.20.Jr, 12.20.Fv

Fifty years of precise comparisons with experiment have established quantum electrodynamics (QED) as the most successful theory in physics. The field is still very active, as shown by recent reports of two hydrogen Lamb shift measurements [1,2] and several new calculations of radiative and recoil corrections [3–7]. This continuing work is motivated by several considerations. First, the fundamental importance of QED requires that it be tested as accurately as possible. Second, new techniques for evaluating QED corrections need to be verified, especially given the importance of QED as a prototype for other quantum field theories. Third, the experiments can lead to improved values for quantities of fundamental interest, such as the proton charge radius and the Rydberg constant. Here we report a new value for the $1S$ Lamb shift in hydrogen. The 6 ppm uncertainty of this result makes it the most precise measurement of a Lamb shift.

Our experiment is based on two-photon laser spectroscopy of the hydrogen $1S$-$2S$ transition [8–10]. This narrow line avoids the broad $2P$ state used in radio-frequency experiments but requires a comparison with a second hydrogen transition to separate the $1S$ Lamb shift from the much larger $1S$-$2S$ Dirac energy. An earlier version of this experiment [11] compared transitions using several intermediate frequency standards and the Rydberg constant. Through a direct comparison of the frequencies of the intervals H($1S$-$2S$) and H($2S$-$4P$), we have now improved on that measurement by a factor of 14.

The apparatus [12] (Fig. 1) uses two tunable ring dye lasers operating near 486 nm. The primary laser is scanned over both the single-photon $2S$-$4P$ transition and (after frequency doubling) the two-photon $1S$-$2S$ transition, while the reference dye laser remains locked to a $^{130}Te_2$ transition located between the two hydrogen lines. The two lasers are heterodyned to measure their frequency difference, giving the ~5 GHz difference frequency H($2S$-$4P$)$-\frac{1}{4}$H($1S$-$2S$). This quantity, which is of course zero in the nonrelativistic Bohr theory, is due to relativistic corrections, hyperfine effects and the Lamb shifts. Since the first two contributions are well understood, this measurement determines a combination of the Lamb shifts of the relevant levels [10].

We now discuss in turn the three major components of the experiment shown in Fig. 1. First, the $1S$-$2S$ spectrometer is an improved version of the system used in Ref. [11]. The required 243 nm radiation is generated by frequency-doubling light from the primary dye laser in a β-barium borate (BBO) crystal inside a power enhancement cavity. The UV light (power ~2 mW) is mode matched with spherical and cylindrical lenses into a nearly confocal power enhancement cavity (buildup factor = 30) which also establishes the counterpropagating beams necessary for Doppler-free excitation. The cavity is placed inside a vacuum chamber, where atomic hydrogen flows through the 105 μm radius waist of the UV standing-wave field. The $1S$-$2S$ resonance [Fig. 2(a)] is detected through the 121 nm fluorescence produced by collisional quenching of atoms excited to the $2S$ level. Most of the data were taken at relatively low pressures (30–50 mTorr), and the line center frequencies were extrapolated to zero pressure with negligible uncertainty (2 kHz) in the pressure shift using the slope of 2.53(7) kHz/mTorr determined from additional data points taken much higher pressures. The extrapolation was checked by using mixtures of helium and hydrogen which gave very different pressure shifts [11].

In the second part of the experiment, the $2S$-$4P$ transition is excited in a beam of metastable $2S$ atoms. Ground state atoms produced in an rf discharge dissociator effuse from a slit into the source chamber of the beam, where

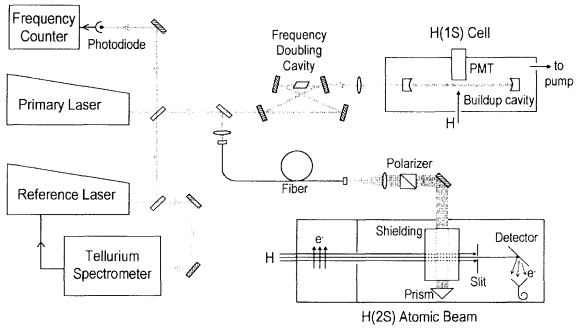

FIG. 1. Schematic diagram of the experimental setup.

 0031-9007/95/75(13)/2470(4)$06.00

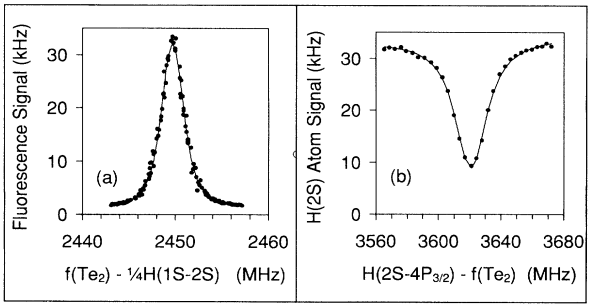

FIG. 2. (a) Typical $1S$-$2S$ spectrum representing 2 min of data collection. The ~2.5 MHz linewidth is due to similar contributions form laser linewidth and the finite transit time of the atoms through the laser beam. (b) Typical $2S$-$4P_{3/2}$ spectrum, representing 5 min of data collective. The ~27 MHz linewidth is due to contributions from the natural width (13 MHz), unresolved hyperfine structure (6 MHz) and residual Doppler broadening.

some are excited to the $2S$ level by a beam of electrons. The atoms then enter a separately pumped chamber, pass through the 486 nm primary laser beam, and strike a gold-coated plate from which the surviving metastable atoms can eject electrons. These are counted with a channel electron multiplier. UV light from the electron bombardment region produces a detector background which is suppressed by modulating the metastable population in the beam with quenching electric field. Since 88% of the atoms excited to the $4P$ state decay rapidly to the ground state, the resonance [Fig. 2(b)] appears as a decrease in the metastable signal. As shown in Fig. 1, the laser beam is aligned at right angle to the collimated atomic beam (divergence = 1 mrad) to reduce the first-order Doppler shift. After crossing the atomic beam the light is retroreflected by a prism with a 90° apex, providing a further suppression since the incident and reflected laser beams are shifted oppositely. There is a small residual shift of the line center because the two beams do not have the same intensity, but we remove this as follows. We take spectra over a small range of atom-laser intersection angles around 90°, using the atomic beam collimating slit to change the angle without disturbing the laser beams. Since the line is Doppler broadened, the minimum in a fit of linewidth to slit position then locates the true 90° position. We then obtain the unshifted transition frequency from a linear fit of spectrum center frequency to slit position. The slope of these fits indicates that the prism suppression factor is 33. For one day of data collection, the uncertainty in the location of the 90° position is 15 μrad. The corresponding random uncertainty in the first-order Doppler shift is 3 kHz, which is negligible compared to the 30 kHz statistical uncertainty in the transition frequency for the same period.

Finally, the reference laser (Fig. 1) is locked to a saturated absorption line in $^{130}Te_2$ [11]. The 15 MHz wide line, 3.88 GHz above the line designated b_2 in Ref. [13], is about half way between the two hydrogen lines at 486 nm. The frequency reproducibility of this system is limited to about 30 kHz by alignment-dependent frequency shifts. These are caused by the saturation of dispersion which must accompany the saturation of absorption of the vapor by the pump beam. As a result, the probe beam is deflected synchronously with the pump beam modulation, acquiring an intensity modulation whose magnitude depends on the particular alignment of the spectrometer. Since the dispersion and the absorption have different frequency response, changes in the spectrometer alignment change the line shape and shift the frequency of the locked reference laser. We avoided the consequences of this effect simply by alternating quickly between the two hydrogen transitions and combining only those pairs of lines taken with the same tellurium spectrometer alignment.

Data collection on a given day alternated between scans over the $F = 1$ to $F = 1$ hyperfine component of H($1S$-$2S$) and one of the two fine structure components of the $2S$-$4P$ line. The polarization of the light driving the $2S$-$4P$ transition was also periodically rotated by 90° to check for systematic shifts discussed below. The final data set consists of 171 $1S$-$2S$ scans and 238 $2S$-$4P$ scans collected over 12 days.

Each scan is fitted with a theoretical line shape, simplified slightly to save computer time in the analysis. For the $1S$-$2S$ transition we use an intensity-normalized Voigt profile with a linear background to allow for detection of scattered 243 nm light. The $2S$-$4P$ profile accounts for saturation, for a slow decrease in the metastable beam intensity, and for the atoms in the $2S$, $F = 0$ state (which are not excited by the laser). In both cases, the fit includes the small measured intensity fluctuations of the laser and it determined the height, width, and center frequency of the resonance for each scan. After each $1S$-$2S$ scan is corrected for the pressure shift, the relevant pairs of line center frequencies are combined and the first-order Doppler shift is dealt with as described above. Combining all of the scans then gives the results shown in the first line of Table I. From these we subtract the Dirac, hyperfine, and relativistic two-body [Eq. (2.3) in Ref. [14]] contributions and correct for the shift associated with atomic recoil from an absorbed photon.

Several systematic corrections are now applied. The small corrections for the second-order Doppler shift are found by fitting our simplified line shapes to complete calculated profiles that include the second-order Doppler shift and the extra weighting of slow atoms because of their longer transit time through the relevant laser beams. We measure the atomic beam velocity distribution by crossing the laser beam at known angles away from 90°, then scanning over the resolved Doppler-shifted peaks. We find that the velocity distribution of the metastable flux can be approximated for our purpose by $P(\nu)d\nu = \nu^n \exp(-M\nu^2/2kT)\,d\nu$, where $n = 5.6(3)$

TABLE I. Reduction of the data.

	$4P_{1/2}$ (kHz)	$4P_{3/2}$ (kHz)
Beat frequencies[a]	4 698 337(12)	6 069 489(9)
Dirac energy	-3 932 893	-5 300 854
Hyperfine structure $(1S, 2S)$	-33 291	-33 291
Relativistic two-body	4186	4186
$2S$-$4P$ photon recoil	-841	-841
$2S$-$4P$ 2nd-order Doppler	50(3)	52(3)
$1S$-$2S$ 2nd-order Doppler	-19(2)	-19(2)
Optical pumping	33(8)	-17(4)
$\frac{1}{4}(\mathcal{L}_{1S} - 5\mathcal{L}_{2S} + 4\mathcal{L}_{4P})$	735 563(15)	738 705(10)
$\mathcal{L}_{1S} - 5\mathcal{L}_{2S} + 4\mathcal{L}_{4P}$	2 942 250(59)	2 954 822(42)
$-4\mathcal{L}_{4P}$ (theory)	5605(1)	-7069(1)
$+5(\mathcal{L}_{2S} - \mathcal{L}_{2P})$[b]	5 289 215(36)	5 289 215(36)
$+5\mathcal{L}_{2P}$ (theory)	-64 175(10)	-64 175(10)
$1S$ Lamb shift, $\mathcal{L}_{1S}$	8 172 896(70)	8 172 792(56)
Combined value for $\mathcal{L}_{1S}$	8 172 827(51)	

[a]Measured values of $H(2S_{F=1}\text{-}4P_J) - \frac{1}{4}H(1S_{F=1}\text{-}2S_{F=1})$.
[b]Weighted average of measurements in Refs. [1,16].

and $T = 289(9)$ K. The uncertainty in the $2S$-$4P$ correction is mostly due to the uncertainty in the beam velocity distribution. For the $1S$-$2S$ correction, we assume that the room-temperature atoms in the interaction volume have a Maxwellian velocity distribution. A numerical simulation shows that the $1S$-$2S$ shift also depends on the laser linewidth. The daily variation in the laser linewidth produces the uncertainty shown in Table I.

Two effects can alter the distribution of atoms among the sublevels of the $2S$ states, changing the intensity ratios of the two $4P$ hyperfine components in each fine structure line from those assumed in our simplified line profiles. This leads to a shift of the fitted line center because the $4P$ hyperfine structure is not resolved. First, spontaneous decays from the $4P$ state to the $2S$ state do not repopulate the four $2S$ magnetic sublevels evenly. We calculate this optical pumping effect by solving the appropriate density matrix equations to find the final $2S$ sublevel populations as a function of laser frequency and then fitting our simplified line shape to these line profiles. The results appear in Table I. Second, in some parts of the electron bombardment region the magnetic field which confines the electron beam is large enough to quench the $F = 1$, $m = -1$, and $F = 0$ states of the $2S$ level by Zeeman shifting them close to the short-lived $2P$ states. However, the resulting polarization does not survive the passage into the magnetically shielded interaction region. As a check of this, we note that an atomic orientation would affect the two fine structure lines very differently and in a way which depends on the laser polarization. Our results (Table II) show no significant dependence on polarization or fine structure component, confirming that this effect is indeed negligible.

Finally, we consider systematic shifts from stray electric and magnetic fields. Atoms in the $2S$-$4P$ interaction region are shielded by a long copper tube (30 cm × 7,5 cm × 2,5 cm), in which the stray field with our oil-free vacuum system is expected to be considerably less [15] than the 20 mV/cm required to give a significant Stark shift (~2 kHz). If there had been a Stark shift, it would be obvious in Table II because the polarizabilities of the $4P_J$ fine structure components have comparable magnitudes but opposite sign. The $1S$-$2S$ transition is less sensitive to electric fields (1 V/cm shifts the $F = 1$ line by only 3.4 kHz), so we expect the shielding provided by the aluminum spacer for the enhancement cavity to be adequate. We verified this by measuring the separation of the two hyperfine components of $H(1S\text{-}2S)$ transition, for which differential Stark shift is $+0.98$ kHz/(V/cm)^2. The measured interval is 4(4) kHz (at 486 nm) smaller than the value inferred from the known hyperfine structure, which is both small and consistent with our expectation of negligible electric field.

Zeeman shifts from stray magnetic fields are even less important: the $1S$-$2S$ shift is insignificant because the levels connected by the $\Delta m = 0$ selection rule have the same g factor, and the $2S$-$4P$ shift is negligible because shielding reduces the residual field to 8 mG.

The remainder of Table I shows the reduction of our measurement of the Lamb shift sum $\mathcal{L}_{1S} - 5\mathcal{L}_{2S} + 4\mathcal{L}_{4P}$ to obtain the ground state Lamb shift $\mathcal{L}_{1S}$ by combining it with the measured $2S$-$2P$ interval [1,16] and the theoretically well-understood P-state Lamb shifts [14]. Figure 3 shows our final result along with the most recent measurement by Hänsch and co-workers [2], derived from a comparison of $H(1S\text{-}2S)$ with the narrow but weak $H(2S\text{-}4S, D)$ transitions. The excellent agreement is important because the two experiments have very different systematic corrections. We believe that the final result in Table I represents the most precise determination of a Lamb shift in any system.

Next we turn to the theory, where two recent review articles [14,17] have already been outdated by new results. The expressions in [14] must be updated to include new calculations of one-loop binding [3], two-loop binding [4,6], pure recoil [5], and radiative-recoil [7] cor-

TABLE II. The data broken down by $2S$-$4P$ fine structure line and laser polarization (column 2: H = horizontal, V = vertical, the atomic beam is horizontal). Column 3: the raw interval measurements. Column 4: these values reduced as in Table I to find the combination of Lamb shifts $\mathcal{L}_{1S} - 5\mathcal{L}_{2S}$. The good agreement between these values confirms that Stark shifts and atomic polarization effects are negligible.

Line	Pol.	$H(2S\text{-}4P_J) - \frac{1}{4}H(1S\text{-}2S)$ (kHz)	$\mathcal{L}_{1S} - 5\mathcal{L}_{2S}$ (kHz)
$2S$-$4P_{1/2}$	H	4 698 341(18)	2 947 870(82)
$2S$-$4P_{1/2}$	V	4 698 333(16)	2 947 841(74)
$2S$-$4P_{3/2}$	H	6 069 483(15)	2 947 727(66)
$2S$-$4P_{3/2}$	V	6 069 493(11)	2 947 768(52)

rections. The $\alpha^2(Z\alpha)^5 m$ two-loop binding correction is particularly important, since two independent calculations show that it contributes -292 kHz to the $1S$ energy, about 30 times more than expected. Although some two-loop binding corrections of order $\alpha^2(Z\alpha)^6 m(\ln Z\alpha)^3$ and $\alpha^2(Z\alpha)^6 m(\ln Z\alpha)^2$ have been calculated recently [18], we do not include them in our theoretical Lamb shifts because other terms of order $\alpha^2(Z\alpha)^6 m$ remain to be calculated. In addition to the QED contributions, the Lamb shift of an S state includes a non-QED correction for the modification of the Coulomb potential inside the nucleus. This is proportional to the mean square radius, which is determined in the case of the proton from ep scattering experiments. Since the two best values, 0.862(12) fm [19] and 0.805(11) fm [20], disagree, we give two calculated values in Fig. 3 for $\mathcal{L}_{1S}$: 8 172 802(40) kHz for the "large" proton and 8 172 654(40) kHz for the "small" proton. The uncertainty reflects similar contributions from the charge radius and from uncalculated or numerically evaluated QED terms. For the sum of Lamb shifts measured directly in our experiment $\mathcal{L}_{1S} - 5\mathcal{L}_{2S} + 4\mathcal{L}_{4P_J}$, the large proton results are 2 942 182(14) and 2 954 856(14) kHz for $J = \frac{1}{2}$ and $\frac{3}{2}$, respectively; using the small proton radius lowers these values by 56 kHz. In all cases our results are in good agreement with the "large proton" theory, but this ambiguity in the proton size stops us making a clean test of the two-loop binding correction even though it is 6 times larger than the uncertainty in our determination of $\mathcal{L}_{1S}$. Obviously a new measurement of the proton size is urgently needed.

Another solution to this problem is to add a third transition to the two already compared, to separate the nuclear size and QED contributions to the Lamb shift. The two-photon $2S$-$4S, D$ transitions in singly ionized helium are particularly suitable for this: the alpha particle size is well known [21], the increase in Z emphasizes the interesting higher-order corrections, and the transition frequency is very close to H($1S$-$2S$), with which it can be compared directly. Further, with the new two-loop binding correction, there is now a nine standard deviation discrepancy between the best experiment [22] and theory for the $He^+(2S$-$2P)$ Lamb shift. To reach the level of this discrepancy one would need to split the $2S$-$4S$ resonance to 15% of its 11 MHz natural width, and work in this direction is now underway in our laboratory. Finally, we note that if a He^+ experiment confirms the QED prediction, the hydrogen result given here determines the proton size. This quantity is now of rather fundamental interest because recent advances in lattice quantum chromodynamics (QCD) suggest that it can be calculated from first principles with an uncertainty of a few percent [23], so that laser spectroscopy of atomic hydrogen could provide a precise test of QCD.

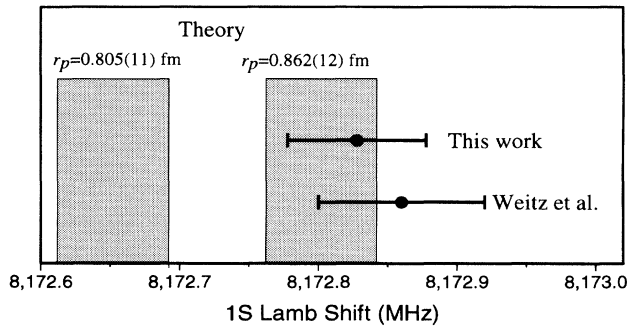

FIG. 3. Comparison of the $1S$ Lamb shift measured in this work, the value 8172.68(6) MHz reported in Ref. [2], and the calculations for the two values of the proton charge radius.

We thank M. D. Plimmer, T. Roach, and K. S. Lai for assistance with this experiment, D. N. Stacey and L. R. Hunter for equipment loans, and K. Pachucki and M. Eides for communicating their results before publication. This work was supported by Yale University, an NIST Precision Measurement grant, and the NSF.

[1] E. W. Hagley and F. M. Pipkin, Phys. Rev. Lett. **72**, 1172 (1994).
[2] M. Weitz, A. Huber, F. Schmidt-Kaler, D. Leibfried, and T. W. Hänsch, Phys. Rev. Lett. **72**, 328 (1994).
[3] K. Pachucki, Ann. Phys. (N.Y.) **226**, 1 (1993).
[4] K. Pachucki, Phys. Rev. Lett. **72**, 3154 (1994).
[5] K. Pachucki and H. Grotch, Phys. Rev. A **51**, 1854 (1995).
[6] M. I. Eides and V. A. Shelyuto, JETP Lett. **61**, 478 (1995).
[7] K. Pachucki, Phys. Rev. A **52**, 1079 (1995).
[8] B. Cagnac, G. Grynberg, and F. Biraben, J. Phys. (France) **34**, 845 (1973).
[9] E. V. Baklanov and V. P. Chebotaev, Opt. Commun. **12**, 312 (1974).
[10] T. W. Hänsch *et al.*, Phys. Rev. Lett. **34**, 307 (1975).
[11] M. G. Boshier *et al.*, Phys. Rev. A **40**, 6169 (1989).
[12] D. J. Berkeland, Ph.D. thesis, Yale University, 1995.
[13] J. R. M. Barr *et al.*, Opt. Commun. **54**, 217 (1985).
[14] J. R. Sapirstein and D. R. Yennie, in *Quantum Electrodynamics,* edited by T. Kinoshita (World Scientific, Singapore, 1990).
[15] E. A. Hessels *et al.*, Phys. Rev. A **46**, 2622 (1992).
[16] S. R. Lundeen and F. M. Pipkin, Phys. Rev. Lett. **46**, 232 (1981).
[17] H. Grotch, Found. Phys. **24**, 249 (1994).
[18] S. Karshenboim, JETP Lett. **79**, 230 (1994).
[19] G. G. Simon *et al.*, Nucl. Phys. **A333**, 381 (1980).
[20] L. N. Hand, D. G. Miller, and R. Wilson, Rev. Mod. Phys. **35**, 335 (1963).
[21] I. Sick, Phys. Lett. B **116**, 212 (1982).
[22] A. van Wijngaarden, J. Kwela, and G. W. F. Drake, Phys. Rev. A **43**, 3325 (1991).
[23] G. P. Lepage (private communication).